Cement and Concrete Research 42 (2012) 1–7

Contents lists available at ScienceDirect

Cement and Concrete Research

journal homepage: http://ees.elsevier.com/CEMCON/default.asp

The effect of supplementary cementitious materials on chloride binding in hardened cement paste

M.D.A. Thomas [a,*], R.D. Hooton [b], A. Scott [c], H. Zibara [b]

[a] Department of Civil Engineering, University of New Brunswick, 17 Dineen Dr., PO Box 4400, Fredericton, New Brunswick, Canada E3B 5A3
[b] Department of Civil Engineering, University of Toronto, 35 St. George St, Toronto, Ontario, Canada M5S 1A4
[c] Department of Civil and Natural Resources Engineering, University of Canterbury, Private Bag 4800, Christchurch, 8140, New Zealand

ARTICLE INFO

Article history:
Received 12 February 2010
Accepted 12 January 2011

Keywords:
Chloride binding
Fly ash (D)
Granulated blast-furnace slag
Silica fume (D)
Metakaolin (D)

ABSTRACT

This paper reports the results of a study to determine the effects of supplementary cementitious materials (SCMs) on the chloride binding of portland cement pastes. The results show that SCMs with significant quantities of alumina increase the binding capacity of cement paste. Pastes with metakaolin (45% Al_2O_3) showed the greatest chloride binding capacity and pastes with silica fume (<0.5% Al_2O_3) showed the least binding. The chemical binding in solutions of high chloride concentration is mainly attributed to the formation of Friedel's salt, $C_3A \cdot CaCl_2 \cdot 10H_2O$. When pastes originally exposed to high chloride concentrations are subsequently exposed to chloride-free solution, a portion of the bound chloride is released, but a significant portion remains irreversibly bound. There is some evidence that Friedel's salt may partially convert to Kuzel's salt, $C_3A \cdot (0.5CaCl_2)(0.5CaSO_4) \cdot 12H_2O$, under these conditions. The binding relationships were best described by the Freundlich isotherm and binding coefficients are given for all the binders tested.

1. Introduction

Supplementary cementitious materials (SCM), such as fly ash, slag, silica fume, and metakaolin and other natural pozzolans, have a significant impact on the ability of concrete to resist the penetration of chloride ions. This benefit is largely ascribed to the refined pore structure that results from the appropriate use of SCM which, in turn, results in reduced permeability and ionic diffusivity. However, SCMs also alter the composition and, hence, the chloride binding capacity of the hydrated phases. Chloride binding has a significant effect on chloride penetration and, hence, on the time to corrosion initiation [1]. It is desirable to include the influence of chloride binding on the chloride penetration process in the modeling of service life for reinforced concrete structures; however, this requires knowledge of the binding isotherms for different types of cementitious materials.

It is known that chlorides react chemically with tricalcium aluminate (C_3A) or its hydrates to form calcium chloro-aluminate, $C_3A \cdot CaCl_2 \cdot 10H_2O$, commonly known as Friedel's salt [2–5]. There is also evidence that physical binding occurs due to the adsorption of chlorides on to the surface of C–S–H [6–10]. The effect of SCMs on chloride binding is varied, with ground granulated blast furnace slag and fly ash generally showing increased chloride binding [11,12] and silica fume showing a decrease in binding capacity [13]. An increase in C–S–H is generally considered to increase chloride binding, yet chloride binding is normally reduced by the addition of silica fume despite an increase in C–S–H. Beaudoin et al. [14] suggest that the degree of chloride binding in C–S–H is a function of the calcium/silica (C/S) ratio with a lower ratio resulting in a lower degree of binding, which may explain the reduction in binding when silica fume is present. Much of the information on chloride binding for binders containing SCM are from studies where chlorides have been introduced at the time of mixing (admixed) and are thus present to react directly with the clinker compounds during hydration. Such an approach likely overestimates the degree of binding that occurs when chlorides are introduced after the binder has hydrated (such as in marine exposures or exposure to de-icer salts) as much of the C_3A will have hydrated and formed relatively stable AFm and AFt phases.

This paper reports results on the effect of SCM on the binding capacity of cement pastes where the chlorides are introduced after hydration. The binding was determined using the equilibrium method developed by Tang and Nilsson [15]. This work forms part of a wider study on the phenomenon of chloride binding conducted by Zibara [16].

2. Experimental methodology

The investigation of the effects of binder type and water-to-cementitious-materials ratio (*w/cm*) on chloride binding involved examining six different SCMs at two *w/cm*. The mixtures included portland cement (meeting the requirements of CSA A3001 Type MS — moderate sulfate-resistant cement) with various replacement levels of SCMs including ternary blends. The SCMs were silica fume,

---

* Corresponding author.
E-mail address: mdat@unb.ca (M.D.A. Thomas).

0008-8846/$ – see front matter © 2011 Elsevier Ltd. All rights reserved.
doi:10.1016/j.cemconres.2011.01.001

metakaolin, blast furnace slag and three fly ashes; the fly ashes were selected to have varying calcium contents to cover the range encountered in North America. The chemical composition of the cementitious materials is provided in Table 1 and the Bogue composition for the cement in Table 2. The mixture proportions of the pastes investigated are presented in Table 3.

All mixes used in this investigation were prepared as pastes containing cementitious materials and distilled water. The *w/cm* ratios were 0.30 and 0.50 with a superplasticiser used for the mixes at *w/cm* = 0.30. The mixes were prepared using a high-speed blender under vacuum to minimize the presence of air bubbles. The paste was cast into 50-mm diameter by 100-mm cylindrical molds. The top of the molds was covered with a plastic sheet followed by a lid which was then sealed with adhesive tape. The molds were rotated at 12 rpm for a period of 24 h to prevent segregation. The paste samples were then cured in sealed molds stored over water at 22 ± 1 °C for a period of 2 months.

At the end of the curing period the pastes were de-molded and the central portion cut into 3-mm thick discs. The sliced samples were then vacuum-dried for three days in a desiccator containing silica gel and soda lime. The dried samples were transferred to a glove box containing soda lime to remove carbon dioxide from the air, and kept at 11% RH for a month. After storage, the 3-mm thick discs were broken into small fragments and samples, weighing approximately 25 g, were placed in 125-mL plastic bottles under vacuum for 2 h. The bottles were then filled with approximately 100 mL of NaCl solution using 7 different concentrations (0.1, 0.3, 0.5, 0.7, 1.0, 2.0, and 3.0 M), sealed and stored at 23 ± 1 °C. The 0.30-*w/cm* samples were stored for 6 months while the 0.50-*w/cm* samples were stored for between 5 and 6 weeks; from preliminary tests, these durations were found to be sufficient to ensure that equilibrium was reached between the pore solution of the samples and the host solution. The host solutions were then analyzed for chloride concentration by means of potentiometric titration using 0.01 M $AgNO_3$.

Selected 0.30-*w/cm* pastes were also stored in NaCl solution at 7 °C and 38 °C in addition to a standard curing temperature of 23 °C; only data from samples stored at 23 °C are reported here. In some cases the number of different chloride concentrations was reduced to three (0.1, 1.0 and 3.0 M) as this was found to be sufficient to establish a binding isotherm [16]. Another variation in the test protocol was that for selected pastes, additional samples were allowed to cure for 9 months prior to the start of the chloride binding tests.

Desorption isotherms were determined for selected 0.50-*w/cm* pastes (OPC, 8SF and 8MK). After equilibrium had been reached in the solution that was initially at 3 M chloride, the solution was removed to determine the equilibrium concentration and the sample was moved to another bottle. Then either 200 mL or 1000 mL of distilled water saturated with $Ca(OH)_2$ (pH = 12.5) was added to the sample. After a storage period of 4 months, to ensure that the sample reached equilibrium with the new solution, the free chloride concentration of the solution was measured.

Table 1
Chemical composition of cement and SCM.

	Portland cement (OPC)	Silica fume (SF)	Meta-kaolin (MK)	Slag (SG)	Fly ash (FA)	Fly ash (FA1)	Fly ash (FA2)
SiO_2	21.26	94.48	52.01	36.18	53.89	43.07	40.82
Al_2O_3	4.09	0.24	44.72	10.02	24.65	20.78	11.09
TiO_2	0.2	0.01	1.6	0.67	1.14	1.10	0.47
P_2O_5	0.07	0.14	0.09	0.01	0.71	0.67	0.10
Fe_2O_3	2.89	0.63	0.58	0.50	8.63	5.41	6.21
CaO	63.58	0.44	0.00	35.49	4.37	17.72	29.89
SrO	0.12	0.02	0.02	0.04	0.16	0.54	0.30
MgO	2.47	0.38	0.00	0.66	0.83	4.18	4.41
Mn_2O_3	0.06	0.03	0.01	13.58	0.05	0.17	0.06
Na_2O_3	0.17	0.16	0.32	0.43	0.6	1.46	1.14
K_2O	0.62	1.01	0.19	0.50	2.14	0.75	1.71
Na_2O_e	0.58	0.82	0.45	0.77	2.07	1.95	2.26
SO_3[a]	2.79	0.36	0.12	1.51	0.61	2.17	2.17
LOI[b]	0.99	2.87	0.9	1.72	1.53	2.57	1.30

[a] SO_3 — based on sulfur determined by LECO.
[b] LOI — loss on ignition at 1000 °C.

Table 2
Bogue cement composition.

	OPC type MS
C_3S	57.6
C_2S	17.6
C_3A	5.9
C_4AF	8.8
Blaine (m^2/kg)	326

3. Results

The use of the equilibrium method assumes that after equilibrium is established between the external solution and the pore solution, the reduction in chloride concentration of the host solution is attributed to chlorides being bound by the cement. The amount of bound chlorides can be determined from:

$$C_b = 35.453 * V * \left(C_i - C_f\right) / W_d \tag{1}$$

where:

C_b	is the amount of bound chloride in mg Cl/g of the sample
V	is the volume of the external solution in mL
C_i	is the initial chloride concentration of the external solution in mol/l
C_f	is the free chloride concentration at equilibrium of the external solution in mol/l
W_d	is the dry mass of the sample in g.

Tests on replicate specimens indicated a low variability and a full discussion on the reproducibility of the test procedure is provided in Zibara [16].

The time to reach equilibrium between the external solution and the pore solution was monitored for a number of samples using a 3-molar chloride solution since it was assumed that the samples with the highest chloride concentration would take the longest to reach equilibrium. The time to reach equilibrium was based on measurements of the chloride concentrations in the external solutions and was found to be a function of both the *w/cm* ratio and the mix composition as shown in Fig. 1. In the case of the 0.50-*w/cm* samples,

Table 3
Details of paste mixtures investigated.

Mix	W/CM	Portland cement (%)	Silica fume (%)	Meta-kaolin (%)	Fly ash (%)	Slag (%)
OPC	0.3, 0.5	100				
8SF	0.3, 0.5	92	8			
8MK	0.3, 0.5	92		8		
25FA	0.3, 0.5	75			25	
25FA1	0.5	75			25	
25FA2	0.5	75			25	
40FA	0.3	60			40	
25SL	0.3, 0.5	75				25
40SL	0.3	60				40
25FA6SF	0.3, 0.5	69	6		25	
40FA5SF	0.3	55	5		40	
25SL6SF	0.3, 0.5	69	6			25
40SL5SF	0.3	55	5			40

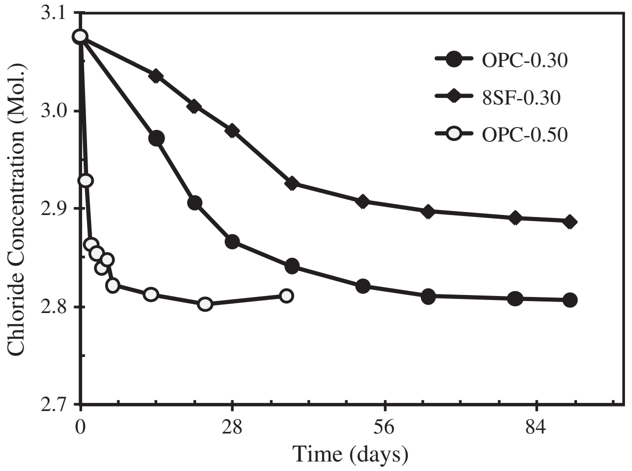

Fig. 1. Time required for chloride concentration of external solutions to reach equilibrium for pastes with OPC (*w*/*cm* = 0.30 and 0.50) and 8% silica fume (*w*/*cm* = 0.30).

the chloride concentration generally started to stabilize after approximately one to two weeks and became constant after three weeks. The use of silica fume, however, resulted in a longer period of approximately three weeks before stabilization, with fairly constant values attained beyond one month. The chloride content of the 0.50-*w*/*cm* samples was determined therefore after six to eight weeks of exposure to chloride solution to ensure that equilibrium was reached. The 0.30-*w*/*cm* samples required a longer stabilization period of approximately one month with fairly constant values attained after two months for the control mix. The chloride concentration of the external solution for the silica fume mix was found to still be decreasing, to a very limited extent, after three month exposure. The chloride concentrations of the 0.30-*w*/*cm* samples were determined after six months to ensure that stable concentrations for all samples were obtained.

Fig. 2 shows the relationship between the bound chloride (C_b) and free chloride (C_f) for the control paste (OPC) with *w*/*cm* = 0.50. The binding is clearly non-linear and the following “best-fit” non-linear isotherms are shown on the same figure:

$$\text{Freundlich isotherm}: C_b = \alpha \cdot C_f^{\beta} \tag{1}$$

$$\text{Langmuir isotherm}: C_b = \frac{\alpha \cdot C_f}{\left(1 + \beta \cdot C_f\right)} \tag{2}$$

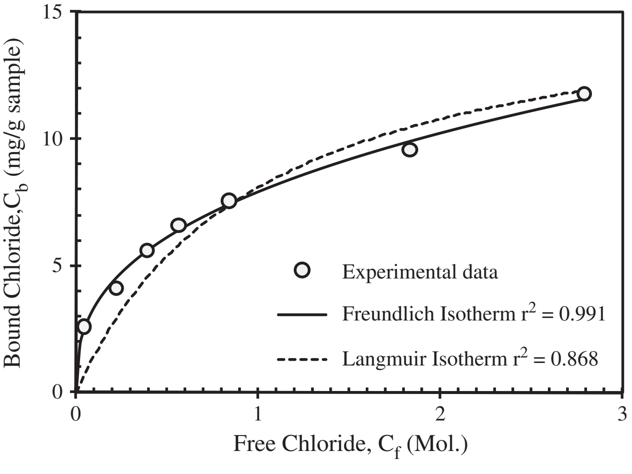

Fig. 2. “Best-fit” isotherms for control paste (OPC) at *w*/*cm* = 0.50.

where α and β are binding constants. The Langmuir isotherm provides a reasonable fit to the experimental data, but in all cases the Freundlich isotherm provided a better fit (higher coefficient of determination). The binding constants for the Freundlich isotherm fitted to the experimental data for all cementitious materials tested are presented in Table 4.

Fig. 3 shows the experimental data and the “best-fit” Freundlich isotherms for three pastes, OPC, 8SF and 8MK, with both 0.30 and 0.50 *w*/*cm*. In general, pastes with 8% silica fume showed the lowest chloride binding and pastes with 8% metakaolin showed the highest binding, compared with all other types of cementitious materials when tested under the same conditions. The increased binding capacity of the paste containing metakaolin is considerable at both *w*/*cm*. The binding capacity increases with *w*/*cm*, especially for the binder containing metakaolin and to a lesser extent for that containing silica fume. The increase for the control paste (OPC) is relatively small.

Fig. 4 shows the effect of fly ash and slag, both at a replacement level of 25%, on the relationship between bound and free chlorides. At *w*/*cm* = 0.30, there is little difference between the control paste (OPC) and the binders with 25% fly ash or slag, but at *w*/*cm* = 0.50 the binding capacity of the fly ash and slag pastes is increased significantly. At higher levels of replacement (40%) both fly ash and slag increased the binding capacity of pastes with *w*/*cm* = 0.30 to a moderate extent (not shown), but unfortunately the study did not include pastes with *w*/*cm* = 0.50 at this higher level of replacement.

The behavior of pastes produced with ternary blends of cementitious materials (portland cement + silica fume + either fly ash or slag as the third component) is shown in Fig. 5. The binding capacity of the ternary blends is slightly lower than the control at *w*/*cm* = 0.30 and slightly higher at *w*/*cm* = 0.50.

Fig. 6 shows that the binding capacity of fly ash (*w*/*cm* = 0.50) varies significantly with different fly ashes. However, there is no trend with calcium content as the fly ash with the intermediate CaO content exhibits significantly higher binding than both the low-CaO and high-CaO fly ashes. Nor can the trend in binding capacity be explained by the total alumina content of the fly ashes.

Fig. 7 shows the effect of extending, from 2 to 9 months, the curing period prior to exposure to chlorides. Little significant or consistent trend was observed with the increased curing period, indicating that evaluation of binding isotherms on 2-month old samples should adequately describe later age isotherms.

XRD analysis of paste samples (*w*/*cm* = 0.50) after they reached equilibrium with the 3-molar chloride solution showed the presence of Friedel's salt, $C_3A \cdot CaCl_2 \cdot 10H_2O$, for all binder types, however, the intensity of the main peak varied significantly as shown in Fig. 8. After immersion in the 3-molar solution, only the control paste (OPC) showed noticeable peaks associated with other AFm and AFt phases;

Table 4
“Best-fit” binding coefficients for Freundlich isotherms.

Binder type	*w*/*cm* = 0.30			*w*/*cm* = 0.50		
	α	β	r^2	α	*B*	r^2
OPC	7.60	0.31	0.999	8.51	0.32	0.994
8SF	4.38	0.33	0.990	6.11	0.37	0.988
8MK	9.84	0.43	0.998	14.9	0.46	0.998
25FA	6.78	0.38	0.998	10.0	0.41	0.977
25FA1				14.1	0.43	0.976
25FA2				9.23	0.35	0.972
40FA	7.55	0.45	0.998			
25SL	7.93	0.30	0.993	10.5	0.39	0.995
40SL	8.62	0.33	0.979			
25FA6SF	4.56	0.59	0.993	7.83	0.47	0.993
40FA5SF	4.77	0.55	0.991			
25SL6SF	5.59	0.43	0.993	8.57	0.40	0.995
40SL5SF	6.25	0.41	0.997			

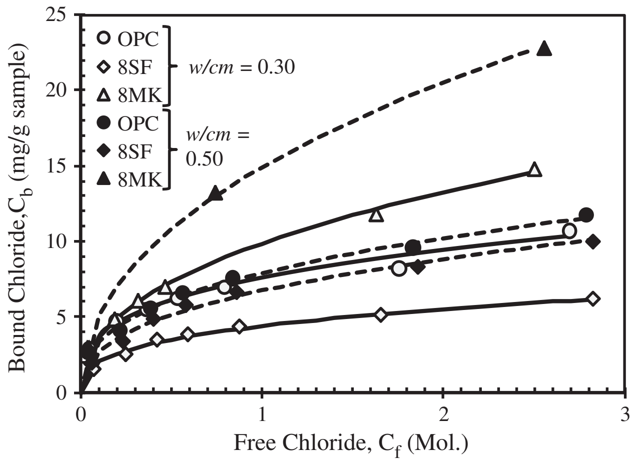

Fig. 3. Chloride binding isotherms for pastes with silica fume and metakaolin (*w*/cm = 0.30 and 0.50, T = 23 °C).

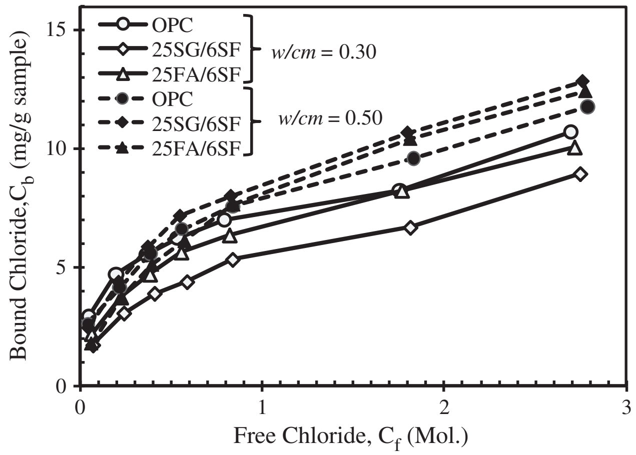

Fig. 5. Chloride binding relationships for ternary cement blends (*w*/*cm* = 0.30 and 0.50, T = 23 °C).

the peaks corresponded to ettringite. Fig. 9 shows a plot of the maximum peak intensity for Friedel's salt (at d = 7.9 Å) against the bound chloride content, C_b, for the pastes after reaching equilibrium with the 3-molar chloride solution. There is a good correlation between these two parameters suggesting that much of the binding that occurs at this high concentration of chloride can be attributed to the formation of Friedel's salt.

The "desorption isotherm" for the paste with 8% metakaolin is shown in Fig. 10 and the results from these tests for all three binders tested are shown in Table 5. After adding 200 mL of chloride-free, saturated $Ca(OH)_2$ solution and allowing equilibrium to be reached, all three binders retained about 80% of the bound chlorides. The chloride concentrations at equilibrium were in the range of 0.12 to 0.14 M. At these chloride concentrations the bound chlorides from the three pastes during sorption were in that range of 3 to 6% (Fig. 2). With a 1000-mL addition, the equilibrium chloride concentration was less than 0.04 M, but still about 40% of the chlorides initially bound after reaching equilibrium with the 3-molar chloride solution remained bound. Fig. 11 shows the results of XRD analysis of the 8MK paste once equilibrium had been reached after the addition of 200 mL and 1000 mL of chloride-free solution. Although the main peak corresponding to Friedel's salt diminishes as the paste reaches equilibrium with the lower chloride concentrations, significant Friedel's salt still remains even when the free chloride falls below 0.04 M. If the bound chloride concentration is estimated from the peak heights shown in Fig. 11 using the relationship shown in Fig. 9, the results yield 14.0 mg/g and 11.8 mg/g, respectively for the 8MK paste after reaching equilibrium with the 200 mL and 1000 mL of chloride-free solution. This compares with 19.2 mg/g and 13.1 mg/g calculated based on the solution equilibrium concentration (Table 5). Fig. 11 shows the presence of a second peak (marked K? in the figures) after the 8MK has reached equilibrium with 1000 mL of chloride-free solution and this peak coincides with the maximum (2-theta) intensity peak of Kuzel's salt, $C_3A\cdot(0.5CaCl_2)(0.5CaSO_4)\cdot 12H_2O$. Kuzel's salt was found at lower chloride concentrations in other parts of this research [16], increasing the likelihood that this peak was indeed Kuzel's salt in this instance.

4. Discussion

The chloride binding capacity of the cement pastes was not only influenced by the composition of the binder but also by the *w*/*cm*. The impact of *w*/*cm* was particularly pronounced for binders containing SCM especially for SCMs that contained large quantities of alumina (e.g. 8MK and, to a lesser extent, 25FA and 25SG). This may indicate that the hydration and pozzolanic reactions are stifled at the lower *w*/*cm* and that much of the alumina present does not become available for the formation of Friedel's salt.

For the 0.50-*w*/*cm* pastes there is clearly a link between the alumina content of the SCM and the extent to which the incorporation

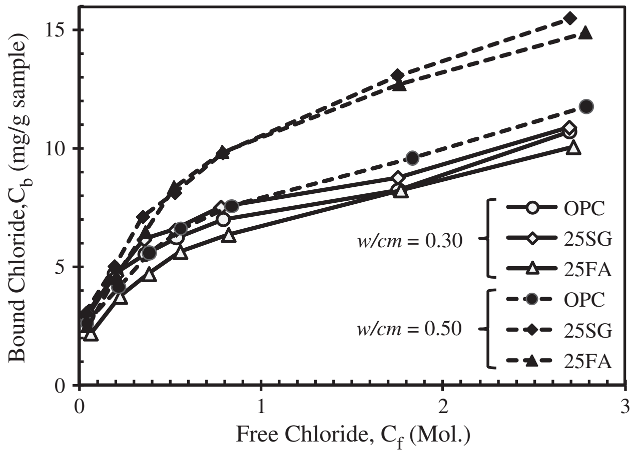

Fig. 4. Chloride binding relationships for fly ash and slag (*w*/*cm* = 0.30 and 0.50, T = 23 °C).

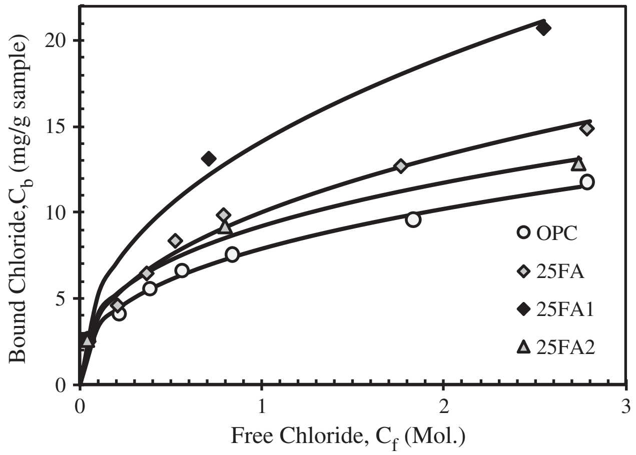

Fig. 6. Chloride binding isotherms for pastes with different fly ashes (*w*/*cm* = 0.50, T = 23 °C).

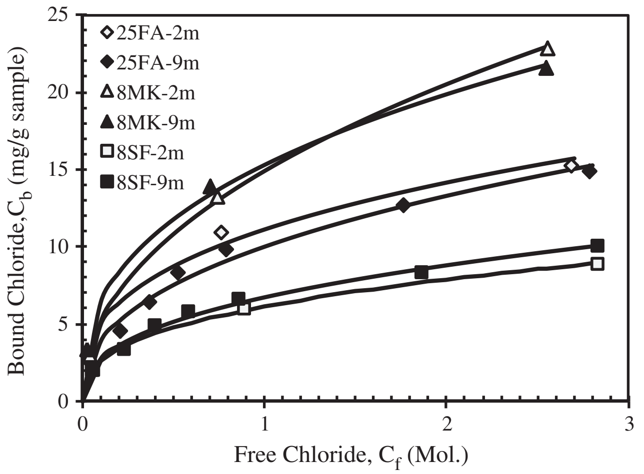

Fig. 7. Chloride binding isotherms for pastes with different fly ashes (*w/cm* = 0.50, T = 23 °C).

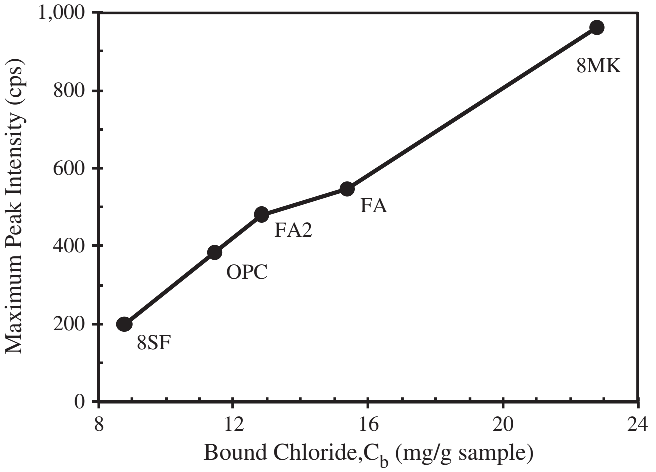

Fig. 9. Relationship between the maximum peak intensity for Friedel's salt (d = 7.9 Å) and the bound chloride of cement pastes after immersion in NaCl solution, $C_i = 3$ M.

of the SCM increases binding, especially at the higher chloride concentrations used in this study. Metakaolin, which comprises approximately 45% Al_2O_3, most of which is assumed to be available, produces the largest increase in the chloride binding capacity, whereas silica fume, which contains a negligible amount of alumina (<0.5% Al_2O_3), actually reduces the binding capacity compared to the control (OPC). Fly ash and slag (10 to 25% Al_2O_3) increase binding but not to the same extent as metakaolin. Fig. 12 shows the relationship between the bound chloride after immersion in NaCl solution ($C_i = 3$ M) and the alumina content of the binder (*w/cm* = 0.50, T = 23 °C). For binders without fly ash, the relationship between these two parameters is clear, however, binders with fly ash do not follow the same relationship. Regarding fly ash, there appears to be no clear criteria, such as total Al_2O_3 or CaO content, that determine its effect on binding. However, much of the alumina in fly ash is present in crystalline components such as mullite, which would not be available to form calcium chloro-aluminates. Consequently, the total alumina content, as reported in Table 1, does not give a reliable indication of how a fly ash will behave with regards to chloride binding. What is required is some measure of the alumina that is "available" and this could be determined using Rietveld quantitative XRD analysis.

The binding capacity of paste containing portland cement plus silica fume (8SF) was lower than that of the control paste (OPC). In addition, the incorporation of 5% silica fume into ternary mixes with 25% fly ash or slag (25FA/5SF and 25SG/5FA) reduced the binding compared with binary mixes with fly ash and slag, but without silica fume (25FA and 25SG). Nilsson et al. [17] suggested that silica fume influences binding in three ways: (i) dilution of the C_3A which may reduce binding, (ii) reduction of the pH of the pore solution which should increase chloride binding, and (iii) and increase in the amount of C–S–H which should increase physical binding of chlorides. The incorporation of silica fume is also known to reduce the C/S ratio of the C–S–H and it has been suggested that this will lead to a reduction in the amount of chloride that can be physically adsorbed onto the surface of the C–S–H [14,18]. Reductions in the C/S ratio of the C–S–H by slag and fly ash also occur, but these SCMs have higher alumina contents and the subsequent formation of C–A–S–H may result in increased binding, in addition to increased formation of Friedel's salt [19]. Experiments by Zibara [16,20] on lime–silica fume pastes confirmed this phenomenon as the chloride binding was observed to decrease as the lime/silica fume ratio decreased. Other workers [21,22] have also observed a reduction in binding due to the presence of silica fume.

The desorption tests indicate that chloride binding is not a completely irreversible process and that a portion of the chlorides that are bound may be released if the free chloride concentration in the pore solution decreases. However, there is significant hysteresis in the absorption–desorption process and a significant quantity of chlorides remains bound, mainly as Freidel's salt, even when the free chloride concentration approaches zero. In other words, a portion of the chemically-bound chlorides is irreversibly bound. The XRD pattern for

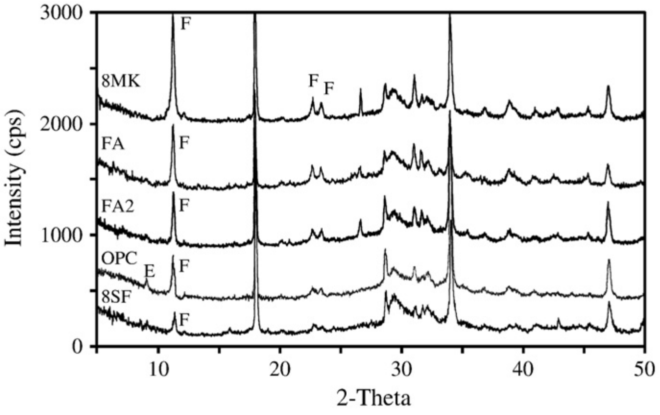

Fig. 8. X-ray diffraction patterns for pastes after immersion in NaCl solution ($C_i = 3$ M) (*w/cm* = 0.50, T = 23 °C) F = Friedel's salt.

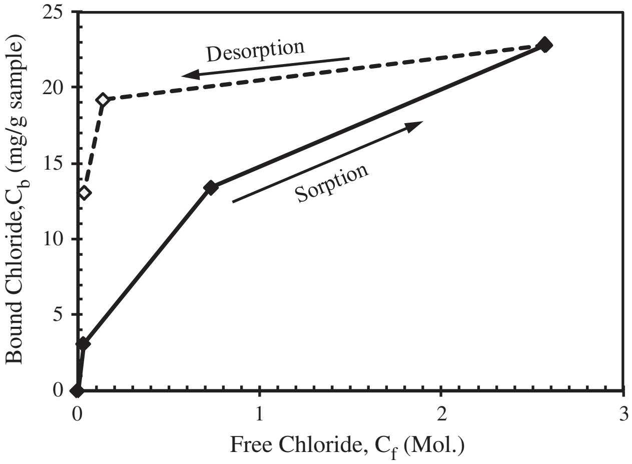

Fig. 10. Chloride "desorption isotherm" for paste with metakaolin (*w/cm* = 0.50, T = 22 °C).

Table 5
Results of desorption tests ($w/cm = 0.50$).

Mixture	Initial $[Cl^-]$ (M)	Water added (mL)	Final $[Cl^-]$ (M)	Initial C_b (mg/g)	Final C_b (mg/g)	Remaining bound (%)
OPC	3.0	200	0.123	11.43	8.73	76
8MK	3.0	200	0.138	22.82	19.21	84
8SF	3.0	200	0.137	8.86	6.92	78
OPC	3.0	1000	0.029	11.2	4.26	38
8MK	3.0	1000	0.035	21.8	13.08	40
8SF	3.0	1000	0.032	7.94	3.14	39

the 8MK after storage in 1000-mL of chloride-free solution revealed the formation of a new peak accompanying the partial dissolution of Friedel's salt. The peak is thought to correspond to Kuzel's salt. The formation of Kuzel's salt at low chloride concentrations (~0.1 M) was confirmed by studies on pure C_3A-gyspum binders by Zibara [16]; he demonstrated the role of chloride concentration (and other factors) on the formation and stability of Kuzel's and Friedel's salt.

5. Conclusions

1. The inclusion of SCM has been shown to affect significantly the chloride binding capacity of the paste. A decrease in the w/cm ratio from 0.50 to 0.30 was generally found to significantly reduce the binding capacity of pastes containing metakaolin, slag, and fly ash.
2. The chloride binding at high free chloride concentrations ($C_f \geq 1.0$ M) is largely due to the formation of Friedel's salt and the amount of binding generally increases with the (available) alumina content of the SCM. The chloride binding was highest with metakaolin (45% Al_2O_3) and lowest with silica fume (<0.5% Al_2O_3).
3. The binding relationships were best described by a Freundlich isotherm.
4. The partial substitution of OPC with 8% silica fume resulted in a significant reduction in the chloride binding capacity at $w/cm = 0.30$ and a smaller reduction at $w/cm = 0.50$. The reduction cannot be explained by the mere dilution of C_3A but must also be a function of the binding capacity of the C–S–H.
5. Fly ash replacement (25%) at $w/cm = 0.50$ showed generally higher binding capacities of fly ashes with varying calcium content compared to the OPC control. No clear relationship, however, existed between the binding capacity and the total calcium or alumina content of the fly ash.
6. If the free chloride content of the pore solution decreases (e.g. due to leaching) a portion of the bound chloride is released, but a significant portion appears to be irreversibly bound.
7. There is some evidence that Kuzel's salt, $C_3A\cdot(0.5CaCl_2)(0.5CaSO_4)\cdot12H_2O$, may form at the expense of Friedel's salt, $C_3A\cdot CaCl_2\cdot10H_2O$, when the paste samples originally exposed to high chloride concentrations are subsequently exposed to chloride-free solution.

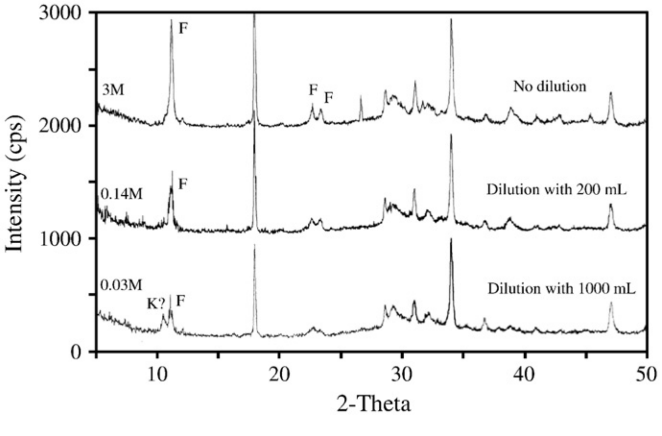

Fig. 11. X-ray diffraction patterns for 8MK pastes after immersion in NaCl solution ($C_i = 3$ M) followed by immersion in different volumes of chloride-free solution ($w/cm = 0.50$, T = 23 °C) F = Friedel's salt, K? = Kuzel's salt?

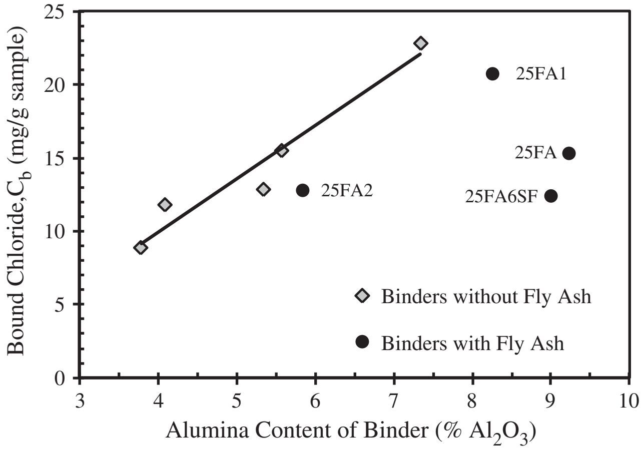

Fig. 12. Relationship between the amount of chloride bound after immersion in NaCl solution ($C_i = 3$ M) and the alumina content of the binder ($w/cm = 0.50$, T = 23 °C).

Acknowledgements

The authors would like to acknowledge the assistance of Dr. S. Petrov, Department of Chemistry, University of Toronto, with the X-ray diffraction testing. Financial support for the research was provided by Materials and Manufacturing Ontario (MMO) and the Natural Science and Engineering Research Council (NSERC) of Canada.

References

[1] B. Martin-Perez, H. Zibara, R.D. Hooton, M.D.A. Thomas, A study of the effect of chloride binding on service life predictions, Cement and Concrete Research 30 (2000) 1215–1223.
[2] M.H. Roberts, Effect of calcium chloride on the durability of pre-tensioned wire in pre-stressed concrete, Magazine of Concrete Research 14 (42) (1962) 143–154.
[3] P.K. Mehta, in: D.E. Tonini, S.W. Dean Jr. (Eds.), Effect of cement composition on corrosion of reinforcing steel in concrete, ASTM STP 629, 1977, pp. 12–19.
[4] S. Diamond, Chloride concentrations in concrete pore solutions resulting from calcium and sodium chloride admixtures, Cement, Concrete and Aggregates 8 (2) (1986) 97–102.
[5] H.F.W. Taylor, Cement Chemistry, 2nd Edition, Academic Press Ltd, London, 1992.
[6] V.S. Ramachandran, Possible states of chloride in the hydration of tricalcium silicate in the presence of calcium chloride, Materiaux et Constructions 4 (19) (1971) 3–12.
[7] V.S. Ramachandran, R.C. Seeley, G.M. Polomark, Free and combined chloride in hydrating cement and cement components, Materiaux et Constructions 17 (100) (1984) 285–289.
[8] G. Blunk, P. Gunkel, H.G. Smolczyk, On the distribution of chloride between the hardening cement paste and its pore solution, 8th International Congress on the Chemistry of Cement, 1986, pp. 85–90.
[9] O. Wowra, M.J. Setzer, Sorption of chlorides on hydrated cements and C3S pastes, in: M.J. Setzer, R. Auberg (Eds.), Frost Resistance of Concrete, E & FN Spon, London, 1997, pp. 147–153.
[10] O. Wowra, M.J. Setzer, About the interaction of chloride and hardened cement paste, 2nd International RILEM Workshop on Testing and Modelling the Chloride Ingress into Concrete, Paris France, 2000.
[11] C. Arya, N.R. Buenfeld, J.B. Newman, Factors influencing chloride binding in concrete, Cement and Concrete Research 20 (2) (1990) 291–300.
[12] R.K. Dhir, M.A.K. El-Mohr, T.D. Dyer, Developing chloride resisting concrete using PFA, Cement and Concrete Research 17 (11) (1997) 1633–1639.
[13] P. Sandberg, J. Larsson, Chloride binding in cement pastes in equilibrium with synthetic pore solution, in: L.O. Nilsson (Ed.), Chloride Penetration into Concrete Structures, Nordic Miniseminar, 1993, pp. 98–107.
[14] J.J. Beaudoin, V.S. Ramachandran, R.F. Feldman, Interaction of chloride and C–S–H, Cement and Concrete Research 20 (6) (1990) 875–883.
[15] L. Tang, L.O. Nilsson, Chloride binding capacity and binding isotherms of OPC pastes and mortars, Cement and Concrete Research 23 (2) (1993) 247–253.
[16] H. Zibara, Binding of external chlorides by cement paste, PhD Thesis, University of Toronto, Canada, 2001, 320 pp.

[17] L.-O. Nilsson, E. Poulson, P. Sandberg, H.E. Sorensen, O. Klinghoffer, in: J.M. Fredriksen (Ed.), HETEK: Chloride Penetration into Concrete, State-of-the-Art, Transport Processes, Corrosion Initiation, Test Methods and Prediction Models, Report, vol. 53, The Road Directorate, Denmark, 1996,, 151 pp.

[18] G.K. Glass, N.M. Hassanein, N.R. Buenfeld, Neural network modelling of chloride binding, Magazine of Concrete Research 49 (181) (1997) 323–335.

[19] S.-U. Hong, F.P. Glasser, Alkali sorption by C–S–H and C–A–S–H gels Part II. Role of alumina, Cement and Concrete Research 32 (2002) 1101–1111.

[20] H. Zibara, R.D. Hooton, M.D.A. Thomas, K. Stanish, Influence of the C/S and C/A ratios of hydration products on the chloride ion binding capacity of lime–SF and lime–MK mixtures, Cement and Concrete Research 38 (2008) 422–426.

[21] C.L. Page, O. Vennesland, Pore solution composition and chloride binding capacity of silica fume cement pastes, Material and Construction 16 (19) (1983) 19–25.

[22] Rasheeduzzafar, S. Ehtesham Hussain, A.S. Al-Gahtani, Pore solution composition and reinforcement corrosion characteristics of microsilica blended cement concrete, Cement and Concrete Research 21 (6) (1991) 1035–1047.